View metadata, citation and similar papers at core.ac.uk

brought to you by CORE

provided by Xiamen University Institutional Repository

The structural properties of wurtzite and rocksalt $Mg_xZn_{1-x}O$

This content has been downloaded from IOPscience. Please scroll down to see the full text.

2008 Semicond. Sci. Technol. 23 025008

(http://iopscience.iop.org/0268-1242/23/2/025008)

View the table of contents for this issue, or go to the journal homepage for more

Download details:

IP Address: 59.77.43.191
This content was downloaded on 12/07/2015 at 03:02

Please note that terms and conditions apply.

Semicond. Sci. Technol. **23** (2008) 025008 (6pp) doi:10.1088/0268-1242/23/2/025008

The structural properties of wurtzite and rocksalt $Mg_xZn_{1-x}O$

Xiaohang Chen and Junyong Kang

Fujian Key Lab of Semiconductor Materials and Applications, Department of Physics, Xiamen University, Xiamen 361005, People's Republic of China

E-mail: jykang@xmu.edu.cn

Received 28 September 2007, in final form 4 December 2007
Published 4 January 2008
Online at stacks.iop.org/SST/23/025008

Abstract

A first principles calculation is used to simulate the variation of the lattice constant, structure, induced charge-density difference, total energy, and band gap of the hexagonal and cubic MgZnO semiconductor alloys with different MgO mole fractions. The calculated results show that the lattice constant and the ratio c/a of the hexagonal $Mg_xZn_{1-x}O$ diminish as the MgO mole fraction is increased, which results in the structure gradually deviating from the wurtzite structure. The angle between the nearest neighbor Zn–O bonds is larger than that between the nearest neighbor Mg–O bonds. The total energy of the hexagonal alloys is lower than, equal to, and larger than that of the cubic one in the lower MgO mole fraction, the MgO mole fraction with 0.69, and the higher MgO mole fraction, respectively. The phase transition is likely to occur as the MgO mole fraction is increased. The crystal structure will become unstable as temperature is raised to a critical value for the different MgO mole fractions no matter what kind the structure is. The band gaps of the hexagonal and cubic $Mg_xZn_{1-x}O$ alloys are the direct type and widen as the MgO mole fraction is increased, which demonstrates that both the structures of the $Mg_xZn_{1-x}O$ alloys are suitable for fabricating the short wavelength devices.

1. Introduction

Due to the wide band gap of 3.37 eV and large exciton binding energy of 60 meV at room temperature, ZnO is considered as a candidate material for the preparation of short wavelength optoelectronic devices, such as from blue to ultraviolet light emitting diodes (LEDs) and laser diodes (LDs). It is expected that the alloying ZnO with MgO can tune the band gap from 3.37 eV to 7.8 eV (MgO band gap), which is essential for band gap engineering as well as heterostructure device design [1]. Since the ionic radius of Mg^{2+} (0.57 Å) is close to that of Zn^{2+} (0.6 Å), the replacement of Zn by Mg should not cause a significant change in lattice constants. According to the phase diagram of the ZnO–MgO ternary system, the thermodynamic solubility limit of MgO in ZnO is less than 4 mol% [2]. Recently, it has been reported that MgZnO films can be grown with MgO compositions up to 33 mol% by using nonequilibrium growth [3–5]. Up to now most studies have focused on the growth and the optical and electrical properties of $Mg_xZn_{1-x}O$ layer or $Mg_xZn_{1-x}O$/ZnO superlattices. However, less attention was paid to the crystal structure.

Generally, a large crystal structure difference between the wurtzite-hexagonal ZnO ($a = 3.25$ Å and $c = 5.21$ Å) and the rock-salt-cubic MgO ($a = 4.21$ Å) can cause unstable phase mixing [3, 6]. It is important to understand the structural characteristics of $Mg_xZn_{1-x}O$ varying with MgO mole fraction. Based on density functional theory (DFT) and some calculative methods of the band gap, *ab initio* simulations have been proved to be useful for the accurate prediction of the crystal characteristics, such as lattice constants [7, 8], phase structure stability [9, 10] and so on. In this work, a first principles calculation is used to investigate the structure stability and some physical parameters of MgZnO alloys with different MgO mole fractions.

2. Model and calculation

The supercells of hexagonal and cubic $Mg_xZn_{1-x}O$ alloys with homogenous distribution are constructed, as shown in figure 1. The hexagonal and cubic $Mg_xZn_{1-x}O$ alloys in the whole composition range are accomplished by increasing the number of the Mg atoms to understand the influence of the different MgO mole fractions on the structure characteristics.

 © 2008 IOP Publishing Ltd Printed in the UK

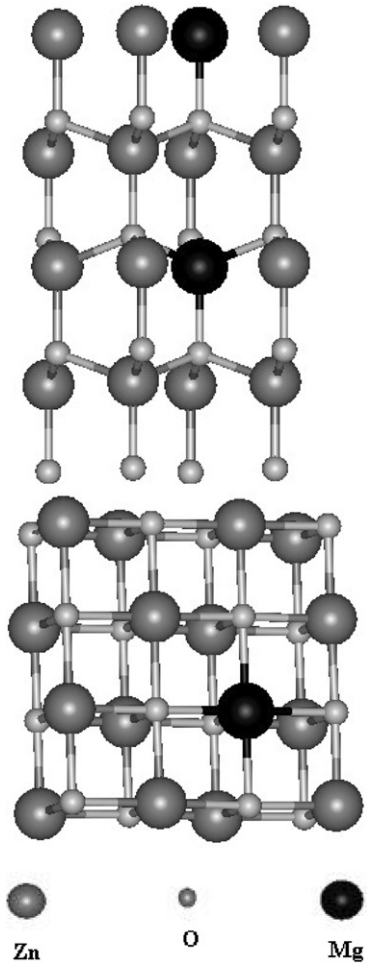

Figure 1. The structural models of the hexagonal (*a*) and cubic (*b*) $Mg_xZn_{1-x}OMg_xZn_{1-x}O$ alloys.

Moreover, the basic characteristics of hexagonal and cubic structures with homogenous distribution of Mg at the same MgO mole fraction are compared in order to know the structure stability.

The Vienna *ab initio* simulation package (VASP) is used to calculate in this paper. VASP is a complex package for performing *ab initio* quantum-mechanical molecular dynamic (MD) simulations by using pseudopotentials and a plane wave basis set. Ionic potentials are represented by ultrasoft pseudopotentials with the Perdew–Wang 1991 (PW1991) generalized gradient approximation (GGA) correction [11, 12]. The wavefunctions are expressed as a supposition of plane waves with a cut-off energy of 395.99 eV. The approach implemented in VASP is based on an exact evaluation of the instantaneous electronic ground states at each MD-step using efficient matrix diagonalization schemes and an efficient Pulay/Broyden charge density mixing. These techniques avoid all problems possibly occurring in the original Car–Parrinello method [13–15]. The geometry optimizations are preformed by relaxing all the degrees of freedom using the conjugate gradient algorithm. The relaxation convergence is 1×10^{-3} eV and 1×10^{-4} eV for ions and electrons, respectively. A $4 \times 4 \times 4$ gamma centred Monkhost–Pack mesh [16] is used to sample the Brillouin zone. Equations of motion at 1136 K and 1500 K have been integrated numerically by using a time step of 4 fs. The MD run has been done in the NVT ensemble.

Table 1. The calculated lattice constants of the hexagonal and cubic $Mg_xZn_{1-x}O$ alloys.

	Lattice constant (Å)			
	Hexagonal $Mg_xZn_{1-x}O$ alloys		Cubic $Mg_xZn_{1-x}O$ alloys	
Mg mole fraction	*a* axis	*c* axis	*a* axis	*c* axis
0.0000	3.2682	5.3340	4.3300	4.3300
0.0625	3.2656	5.2941	4.3244	4.3208
0.1250	3.2630	5.2783	4.3188	4.3144
0.1875	3.2589	5.2764	4.3131	4.3118
0.2500	3.2569	5.2610	4.3075	4.3078
0.3125	3.2553	5.2498	4.3019	4.3027
0.3750	3.2527	5.2446	4.2963	4.2965
0.4375	3.2501	5.2338	4.2906	4.3186
0.5000	3.2475	5.2182	4.2850	4.2879
0.5625	3.2449	5.2093	4.2794	4.2842
0.6250	3.2424	5.2009	4.2738	4.2753
0.6875	3.2398	5.1774	4.2681	4.2691
0.7500	3.2371	5.1623	4.2625	4.2642
0.8125	3.2325	5.1466	4.2569	4.2661
0.8750	3.2320	5.1293	4.2513	4.2565
0.9375	3.2294	5.0969	4.2456	4.2488
1.000	3.2268	5.0449	4.2400	4.2400

3. Results and discussion

By comparing the calculated data of the supercells of $Mg_xZn_{1-x}O$ with 64 and 32 atoms, the changes of their basic parameters, such as the lattice constant, band gap and so on, have not been observed within computing error (less than 1%). Thus, the supercell with 32 atoms is used in the following calculation.

The lattice constants of the hexagonal and cubic $Mg_xZn_{1-x}O$ alloys with homogenous distribution of Mg are calculated in the whole composition range. The calculated lattice constants of the hexagonal and cubic $Mg_xZn_{1-x}O$ alloys with different MgO mole fractions are listed in table 1. It is seen that the lattice constants in the *a* and *c* axes of the two structures diminish as the MgO mole fraction is increased. This variation trend agrees with the experiment results of the hexagonal and cubic $Mg_xZn_{1-x}O$ alloys [3, 17]. Generally, the variation of the lattice constant is attributable to the bond flex of anion and cation, radius difference of substitutional ion, and change of the crystal structure. Since the ionic radius of Mg^{2+} (0.57 Å) is smaller than that of Zn^{2+} (0.6 Å), the lattice constant decreases as the MgO mole fraction is increased. At the same time, it is interesting to note that when the MgO mole fraction is increased, the lattice constant will increase, because Mg–O bond is longer than Zn–O bond. On the other hand, the increase of the MgO mole fraction may cause the structure adjustment, which results in the decrease of the lattice constant.

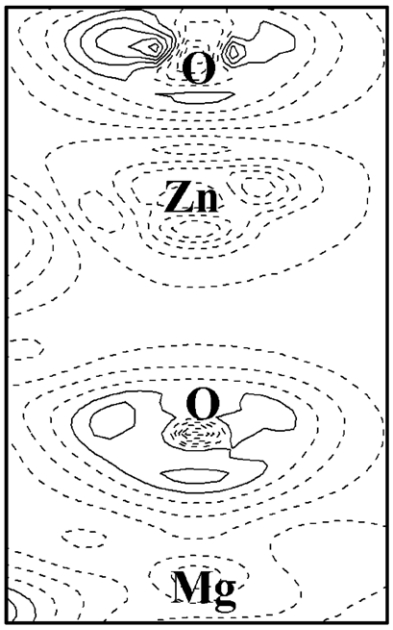

Figure 2. The charge-density differences on a cross section of the hexagonal MgZnO alloy.

Because the stable phase of ZnO is the hexagonal structure while that of the MgO is the cubic one, the structure phase should change from hexagonal to cubic when the MgO mole fraction exceeds some value. It is found that the c/a ratio of the hexagonal $Mg_xZn_{1-x}O$ diminishes as the MgO mole fraction is increased. Simultaneously, by comparing the atom positions before and after relaxation, it can be seen that the atoms surrounding substitutional Mg atom relax outward. The relaxation magnitude increases with the increase of the MgO mole fraction and reaches up to 1.5–2.0% and 1.2–1.6% along the a and c axes, respectively. As a result of the relaxation anisotropy, the angle between the bonds changes up to 9° and causes $Mg_xZn_{1-x}O$ deviating from wurtzite structure gradually. The above discussion shows that there is a tendency, i.e., the configuration of the $Mg_xZn_{1-x}O$ alloys deviates from the hexagonal as the MgO mole fraction is increased.

The induced charge-density differences are calculated to understand the structure deviation. Figure 2 shows a cross section of the induced charge-density differences for the hexagonal $Mg_xZn_{1-x}O$ alloys, where the regions of increased and decreased charge densities are represented by the solid and dashed lines, respectively. It is found that there is a spike of the distribution of the induced charge-density differences along the Mg–O bond while it is invisible along the Zn–O bond. It is reasonable that when the Mg and Zn atoms respectively bond to the O atom, the Mg atom will lose electrons more easily than the Zn atom because the Pauling electronegativities, 1.31, of Mg is smaller than that, 1.65, of the Zn. At the same time, it can be seen that the angle between the nearest neighbor Zn–O bonds is larger than that between the nearest neighbor Mg–O bonds. It can be attributed to the stronger interaction between the second nearest neighbor Mg–O bonds due to the stronger polarity of the Mg–O bonds. In the light of the above discussion, one can come to a conclusion: the crystal structure will deviate from wurtzite gradually as the quantity of the Mg–O bond is increased.

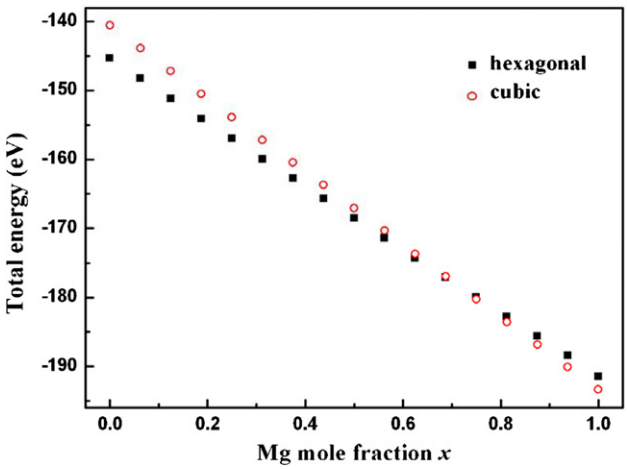

Figure 3. The total energies of the hexagonal (square) and cubic (circular) $Mg_xZn_{1-x}O$ alloys.

Furthermore, the total energy of the system reduces as the MgO mole fraction is increased. Figure 3 shows the total energy of the hexagonal and cubic $Mg_xZn_{1-x}O$ alloys with the different values of x varying from 0.000 to 1.000. Since the decreasing rate of the total energy of the hexagonal structure is smaller than that of the cubic one, the total energy of the hexagonal alloys is lower than, equal to, and larger than that of the cubic one in the lower MgO mole fraction, the MgO mole fraction with 0.69, and the higher MgO mole fraction, respectively. This indicates that the hexagonal structure is more stable when the MgO mole fraction is smaller than 0.69, while the cubic structure is more stable when the MgO mole fraction is larger than 0.69. Generally, the change of the crystal structure usually relates to the phase transition or phase separation as the MgO mole fraction is increased. In order to know the structural variation of the hexagonal and cubic $Mg_xZn_{1-x}O$ alloys, one should further calculate the molar mixing free energies of the hexagonal and cubic $Mg_xZn_{1-x}O$ alloys, which can be approximately expressed as

$$\Delta F(x) = \mathrm{F}_{\mathrm{Mg}_x\mathrm{Zn}_{1-x}\mathrm{O}} - [x\mathrm{F}_{\mathrm{MgO}} + (1-x)\mathrm{F}_{\mathrm{ZnO}}], \qquad (1)$$

where $\mathrm{F}_{\mathrm{Mg}_x\mathrm{Zn}_{1-x}\mathrm{O}}$, $\mathrm{F}_{\mathrm{MgO}}$ and $\mathrm{F}_{\mathrm{ZnO}}$ represent the free energy of the alloys, MgO and ZnO, respectively. The mixing free energy is determined by the total energy at 0 K. Since the sign and magnitude of the mixing free energy of the $Mg_xZn_{1-x}O$ system can be used to infer the structure stability, the composition dependences of $\Delta F(x)$ of the hexagonal and cubic $Mg_xZn_{1-x}O$ alloys are shown in figure 4. The curves of $\Delta F(x)$ exhibit that there is only a minimum in the whole composition range for both the hexagonal and the cubic structure. As we know, the phase separation is possibly to occur if the curves of $\Delta F(x)$ have minima at ZnO and MgO. In our case, the possibility of the phase transition will be higher than that of the phase separation as the MgO mole fraction is increased. It is believed that when the MgO mole fraction is increased, the structure of the $Mg_xZn_{1-x}O$ alloy

Table 2. The total energies of the hexagonal and cubic $Mg_xZn_{1-x}O$ alloys in the different temperatures.

	Total energy (eV)			
	Hexagonal structure		Cubic structure	
Temperature (K)	$x = 0.6250$	$x = 0.7500$	$x = 0.6250$	$x = 0.7500$
0	−174.2802	−179.9414	−173.6715	−180.2395
1136	−169.1579	−172.1241	−169.5800	−172.8904
1500	−167.4517	−171.6798	−167.6941	−171.6020

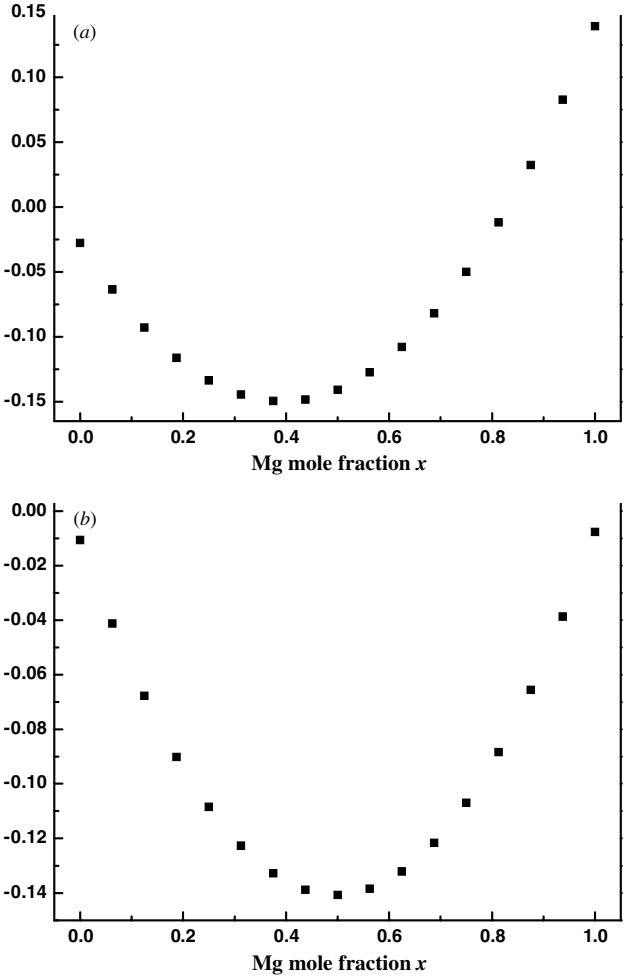

Figure 4. The molar mixing free energies of the hexagonal (*a*) and cubic (*b*) $Mg_xZn_{1-x}O$ alloys.

will change, and consequently, the phase transition from the wurtzite to cubic structure may occur. It has been reported [3, 18] that by varying the MgO composition, the band gap can be tuned from 3.3 eV to 7.8 eV for the hexagonal and cubic $Mg_xZn_{1-x}O$ alloys, extending the cutoff wavelength from UV-A (320–400 nm) to UV-B (280–320 nm) and UV-C (200–280 nm) regions. Thus, choosing a reasonable MgO mole fraction, one can obtain the right structure of the $Mg_xZn_{1-x}O$ alloys, which have many applications such as solar UV radiation, ultra-high temperature flame detection and airborne missile warning systems.

Generally, the phase stability is also closely related to the temperature as well as alloy composition. The phase stability of the hexagonal and cubic structures is compared with the calculated total energies of the different MgO mole fractions of 0.6250 and 0.7500 at different temperatures. Because the energy fluctuation of this small simulated cell will be inevitably high, the energies from *ab initio* MD are averaged over 250 time steps for high temperature to reduce the calculation error less than 1%. As listed in table 2, the total energy for the same structure with the same composition raises as the temperature is increased due to the enhancement of the thermal motion of atoms. The total energy of the cubic structure turns out to be smaller than that of the hexagonal one with the MgO mole fraction of 0.6250 at the temperature of 1136 K, even though it is larger at the temperature of 0 K. For the higher MgO mole fraction of 0.7500, the turning point of the total energy occurs at the higher temperature of 1500 K. According to the fundamental relation of thermodynamics, one has

$$\Delta G = \Delta U - T\Delta S + P\Delta V, \tag{2}$$

where G, U, T, S, P and V are the Gibbs free energy, total energy, temperature, entropy, pressure and volume, respectively. Since the simulated crystals are assumed in vacuum ($P = 0$), equation (2) can be simplified as

$$\Delta G = \Delta U - T\Delta S. \tag{3}$$

The contribution of entropy comes into play an important role at high temperatures. As we know, the entropy as well as the total energy will increase as the temperature rises. As a result, the Gibbs free energy of both the structures will become large. It means that the crystal structure maybe become unstable as temperature rises to a critical value no matter what kind of the structure is. Although the critical values of the total energies at different high temperatures have been calculated, the critical values of entropies of the two phase structures with different MgO mole fractions are impossible to calculate with VASP (only the electronic entropy is included in S and the configurational and vibrational contributions are not accounted for). According to the experimental observation, the structural transition of $Mg_xZn_{1-x}O$ from hexagonal to cubic phase occurs in the temperature range of 750 °C to room temperature for MgO mole fraction $x = 0.5$ [19], while the calculated total energy of the hexagonal structure is lower than that of the cubic one, which indicates that the entropy of the cubic structure may be larger than that of the hexagonal one at the same high temperature.

It is interesting to note that the band gap of the hexagonal alloys is wider than that of the cubic one with the lower MgO mole fraction and changeovers to the narrower one at the MgO mole fraction of 0.69 at 0 K. This is likely to imply that the electronic structures of $Mg_xZn_{1-x}O$ have a critical

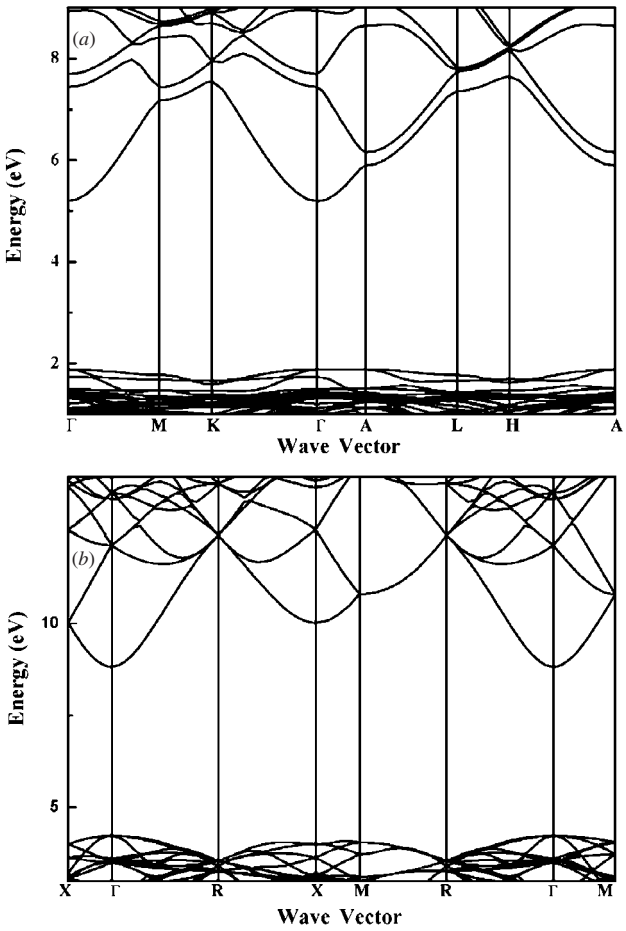

Figure 5. The band structures of the hexagonal (*a*) and cubic (*b*) MgZnO alloys.

point. To understand the composition dependence of the electronic structure, the band structures of the hexagonal and cubic $Mg_xZn_{1-x}O$ are calculated at 0 K. The composition dependences of band gaps of the hexagonal and cubic $Mg_xZn_{1-x}O$ alloys enlarge as the MgO mole fraction is increased. It agrees with the experimental results [20, 21], which show that the band gaps of the hexagonal and cubic $Mg_xZn_{1-x}O$ alloys increase about 1.01 eV and 2.40 eV when x is varied form 0 to 0.4 and from 0.6 to 1, respectively. However, the calculated band gaps in both the structures are smaller than the experimental values due to the underestimation of the band gap with the local-density approximation (LDA) [22], the raise of the valence band with GGA [20] and the strong locality of the d states of Zn. Furthermore, the top of the valence band and the bottom of the conduction band appear at the same k-point of Γ for both the structures no matter what the mole fraction of MgO is, as show in figure 5, which indicates that both structures of $Mg_xZn_{1-x}O$ are the direct band-gap semiconductors. Since the direct band-gap semiconductors have more advantages for high emission possibility, the characteristics of direct band gap for both structures allow people to select different types of structures with the different MgO mole fractions to fabricate optoelectronic devices.

It is well known that the more flexural the top of the valence band and the bottom of the conduction band are, the less the effective masses of holes and electrons, and the higher the mobilities of holes and electrons. The calculated band structures illustrate that the curvatures of the top of the valence band and the bottom of the conduction band gradually become small as the MgO mole fraction is increased. It means that the mobility in the alloys will fall when the MgO mole fraction is increased. For this reason, the change of the mobility must be taken into account when the higher MgO mole fraction is used to modulate the band gap.

4. Conclusions

VASP has been used to investigate the various performances of the hexagonal and cubic MgZnO semiconductor alloys with different MgO mole fractions. The calculated results show that an increase of the MgO mole fraction will reduce the lattice constant and the ratio c/a of the hexagonal $Mg_xZn_{1-x}O$, and consequently, result in the structure of $Mg_xZn_{1-x}O$ deviating from wurtzite structure gradually. The structure deviation can be attributed to the stronger interaction between the second nearest neighbor Mg–O bonds due to the stronger polarity of the Mg–O bonds. When the MgO mole fraction is increased, the total energies of both the structures of the $Mg_xZn_{1-x}O$ alloys reduce. The reduction rate of the total energy of the cubic alloy is larger than that of the hexagonal one and the total energies of both the structures are the same for the MgO mole fraction of 0.69. This indicates that the hexagonal structure is more stable for a small MgO mole fraction while the cubic one is more stable for a large MgO mole fraction. The molar mixing free energies of the hexagonal and cubic $Mg_xZn_{1-x}O$ alloys are calculated to investigate the possibility of the phase transition or phase separation. The results imply that the phase transition is likely to occur as the MgO mole fraction is increased. The phase transitions between the hexagonal and cubic structures can be evaluated by calculating the total energies of the different MgO mole fractions at different temperatures. The crystal structure will become unstable as temperature rises to a critical value for the different MgO mole fractions no matter what kind the structure is. The growth temperature should be lower than the critical point and the MgO mole fraction should be away from 0.69 in order to grow $Mg_xZn_{1-x}O$ alloys free from phase mixing.

Acknowledgments

This work was supported by the National Natural Science Funds (60336020) and the Science and Technology Programs of Xiamen (3502Z20063001), People's Republic of China.

References

[1] Bagnall D M, Chen Y F, Zhu Z, Yao T, Koyama S, Shen M Y and Goto T 1997 *Appl. Phys. Lett.* **70** 2230–2
[2] Sarver J F, Katnack F L and Hummel F A J 1959 *Electrochem. Soc.* **106** 960

[3] Ohtomo A, Kawasaki M, Koida T, Masubuchi K, Koinuma H, Sakurai Y, Yoshida Y, Yasuda T and Segawa Y 1998 *Appl. Phys. Lett.* **72** 2466–8
[4] Heo Y W, Tien L C and Norton D P 2005 *J. Mater. Res.* **20** 3028–33
[5] Kim J H, Kim B, Andeen D and Lange F F 2007 *J. Mater. Res.* **22** 943–9
[6] Park W I, Yi G C and Jang H M 2001 *Appl. Phys. Lett.* **79** 2022–4
[7] Erhart P, Klein A and Albe K 2005 *Phys. Rev.* B **72** 085213
[8] Erhart P, Albe K and Klein A 2006 *Phys. Rev.* B **73** 205203
[9] Zhimei S, Jian Z and Ahuja R 2006 *Phys. Rev. Lett.* **96** 055507
[10] Sanati M, Hart G L W and Zunger A 2003 *Phys. Rev.* B **68** 155210
[11] Perdew J P, Chevary J A, Vosko S H, Jackson K A, Mark R P, Singh D J and Carlos F 1992 *Phys. Rev.* B **46** 6671–87
[12] Wang Y and Perdew J P 1991 *Phys. Rev.* B **44** 13298–307
[13] Kresse G and Furthmuller J 1996 *Phys. Rev.* B **54** 11169–86
[14] Kresse G and Furthmuller J 1996 *Comput. Mater. Sci.* **6** 15–50
[15] Kresse G and Furthmuller J 1999 *Phys. Rev.* B **59** 1758–75
[16] Monkhost H J and Park J D 1977 *Phys. Rev.* B **13** 125188
[17] Lu Y M, Wu C X, Wei Z P, Zhang Z Z, Zhao D X, Zhang J Y, Liu Y C, Shen D Z and Fan X W 2005 *J. Cryst. Growth* **278** 299–304
[18] Teng C W, Muth J F, Ozgur U, Bergmann M J, Everitt H O, Sharmar A K, Jin C and Narayan J 2000 *Appl. Phys. Lett.* **76** 979–81
[19] Choopun S, Vispute R D, Yang W, Sharma R P and Venkatesan T 2002 *Appl. Phys. Lett.* **80** 1529–31
[20] Jaffe J E, Snyder J A, Lin Z J and Hess A C 2000 *Phys. Rev.* B **62** 1660–5
[21] Takeuchi I, Yang W, Chang K S, Aronova M A, Venkatesan T, Vispute R D and Bendersky L A 2003 *J. Appl. Phys.* **94** 7336–40
[22] Fan W J, Abiyasa A P, Tan S T, Tan S F, Yu S F, Sun X W, Xia J B, Yeo Y C, Li M F and Chong T C 2006 *J. Cryst. Growth* **287** 28–33